

Special Report 89-17

April 1960

*(Handwritten circled number 12)*  
*(Handwritten signature)*

# INFLUENCE OF NOSE SHAPE AND L/D RATIO ON PROJECTILE PENETRATION IN FROZEN SOIL

Paul W. Richmond

20000727242

ADA 085398

DTIC  
SELECTED  
JUN 12 1960  
A

Reproduced From  
Best Available Copy

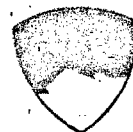
DDG FILE COPY

Prepared for  
DIRECTORATE OF MILITARY CONSTRUCTION  
OFFICE OF THE CHIEF OF ENGINEERS

By



UNITED STATES ARMY  
CORPS OF ENGINEERS  
COLD REGIONS RESEARCH AND ENGINEERING LABORATORY  
HANOVER, NEW HAMPSHIRE, U.S.A.



Approved for public release. Distribution unlimited.

80 6 12 103

Unclassified

SECURITY CLASSIFICATION OF THIS PAGE (When Data Entered)

REPORT DOCUMENTATION PAGE		READ INSTRUCTIONS BEFORE COMPLETING FORM
1. REPORT NUMBER Special Report, 80-17	2. GOVT ACCESSION NO. AD-A085398	3. RECIPIENT'S CATALOG NUMBER
4. TITLE (and Subtitle) INFLUENCE OF NOSE SHAPE AND L/D RATIO ON PROJEC- TILE PENETRATION IN FROZEN SOIL	5. TYPE OF REPORT & PERIOD COVERED	
7. AUTHOR(s) Paul W. Richmond	6. PERFORMING ORG. REPORT NUMBER	
9. PERFORMING ORGANIZATION NAME AND ADDRESS U.S. Army Cold Regions Research and Engineering Laboratory Hanover, New Hampshire 03755	8. CONTRACT OR GRANT NUMBER(s)	
11. CONTROLLING OFFICE NAME AND ADDRESS Directorate of Military Construction Office of the Chief of Engineers Washington, DC 20341	12. REPORT DATE Apr 1980	10. PROGRAM ELEMENT, PROJECT, TASK AREA & WORK UNIT NUMBERS DA Project/4A762738AT42 Task A1, Work Unit 007
14. MONITORING AGENCY NAME & ADDRESS (if different from Controlling Office)	13. NUMBER OF PAGES 27	15. SECURITY CLASS. (of this report) Unclassified
16. DISTRIBUTION STATEMENT (of this Report) Approved for public release; distribution unlimited.	15a. DECLASSIFICATION/DOWNGRADING SCHEDULE	17. A 1
17. DISTRIBUTION STATEMENT (of the abstract entered in Block 20, if different from Report)	14 CRREL-SR-80-17	
18. SUPPLEMENTARY NOTES		
19. KEY WORDS (Continue on reverse side if necessary and identify by block number) Cold regions Laboratory tests Penetration Sabot projectiles Silt		
20. ABSTRACT (Continue on reverse side if necessary and identify by block number) This report presents the results of a laboratory test program designed to deter- mine the applicability of two analytical solutions to projectile penetrations in frozen soils. The test program consisted of firing small caliber cylindri- cal projectiles into frozen soil targets. Four types of 7.9-mm-diam projectiles were tested: two with a hemispherical nose the other two flat-nosed, with both long (length/diameter = 4) and short (L/D = 2) versions of each nose shape. Penetration depth versus impact velocity data are presented. Comparisons of		

037100

GM

Unclassified

SECURITY CLASSIFICATION OF THIS PAGE (When Data Entered)

20. (cont'd).

the data indicate that a flat-nosed projectile is a less efficient penetrator than one of equal weight with a hemispherical nose. A small increase in resistance to penetration is observed for an increased L/D ratio. Two penetration solutions are compared with the test results. One is empirical, based on target strength and projectile characteristics. The other, a closed form solution, is based on the expansion of a spherical cavity in the target material. Modifications and further definition of nose shape coefficients and a mass scaling factor increase the applicability and accuracy of the empirical method to the solution of small arms penetration problems. The closed form solution performed well for impact velocities below 600 m/s.

Unclassified

SECURITY CLASSIFICATION OF THIS PAGE (When Data Entered)

PREFACE

This report was prepared by Paul W. Richmond, Mechanical Engineer, Civil Engineering Research Branch, Experimental Engineering Division, U.S. Army Cold Regions Research and Engineering Laboratory.

The study was funded under DA Project 4A762730AT42, Design, Construction, and Operations Technology for Cold Regions; Task A1, Ice and Snow Technology; Work Unit 007, Projectile and Fragment Attenuation in Cold Regions Materials.

The author thanks Dennis R. Farrell for his suggestions and guidance in performing the laboratory tests, and George W. Aitken, Dr. George Swinzow, and David M. Cole who technically reviewed the report.

The contents of this report are not to be used for advertising or promotional purposes. Citation of brand names does not constitute an official endorsement or approval of the use of such commercial products.

Disc  
A

CONTENTS

	<u>Page</u>
Abstract. . . . .	1
Preface . . . . .	iii
Introduction. . . . .	1
Test Program. . . . .	1
Discussion of Results . . . . .	5
General. . . . .	5
Nose Shape Effect. . . . .	10
L/D Influence. . . . .	10
Target Temperature Effects . . . . .	12
Penetration Estimates . . . . .	12
General. . . . .	12
Sandia Equation. . . . .	13
Spherical Cavity Expansion Technique . . . . .	15
Conclusions . . . . .	20
Literature Cited. . . . .	21

ILLUSTRATIONS

Figure

1.	CRREL Terminal Ballistics Facility . . . . .	2
2.	Projectiles tested . . . . .	2
3.	Test round components . . . . .	3
4.	Propellant load versus velocity data . . . . .	3
5.	Characteristics of the Hanover silt used as a target material (LL=44.8, PL=non plastic, optimum water content=21.0%, $G_s=2.69$ ) . . . . .	4
6.	Dissected target . . . . .	8
7.	Large (L/D = 4) projectile sabot and modifications ..	9
8.	Small (L/D = 2) projectile sabot and modifications ..	9

9. Nose shape influence on penetration of equal mass projectiles (the solid lines are least square curve fits to the data) . . . . . 11

10. Effect of L/D ratio and mass on flat nose projectile penetration (the solid lines are least square curve fits to the data) . . . . . 11

11. Effect of frozen soil temperature on projectile penetration (the solid lines are least square curve fits to the data) . . . . . 12

12. Comparison of test data with penetration solutions, for the flat-nose, L/D = 2 projectile, target at -10°C . . . . . 16

13. Comparison of test data with penetration solutions, for the flat-nose, L/D = 2 projectile, target at -25°C . . . . . 16

14. Comparison of test data with penetration solutions, for the hemispherical nose, L/D = 2 projectile, target at -10°C . . . . . 16

15. Comparison of test data with penetration solutions, for the flat-nose, L/D = 4 projectile, target at -10°C . . . . . 17

16. Relation between projectile mass and mass scaling factor K . . . . . 17

17. Idealized strain curve for spherical cavity expansion theory . . . . . 17

Table

1. Description of projectiles . . . . . 5

2. Penetration data . . . . . 6

3. Nose performance coefficient . . . . . 14

4. Typical soil constants for natural earth materials . . . . . 15

## INTRODUCTION

Numerous tests have been conducted by various agencies in an attempt to understand the fundamental mechanics of earth penetration by projectiles (Bernard 1975). Several empirical and semi-empirical equations as well as finite difference methods have been used to estimate projectile penetration in earth material. This report presents the results of a laboratory test program conducted to determine the applicability of two of the more widely used solutions to the problem of projectile penetration of frozen soil.

The test program consisted of firing small caliber cylindrical projectiles into frozen Hanover silt. Projectiles with two different length to diameter (L/D) ratios (2 and 4) and two nose shapes (flat and hemispherical) were used in the test program. Measurements of projectile penetration and impact velocity were made and soil properties documented.

Penetration depth versus impact velocity data are presented. Comparisons of least square curve fits of the data indicated that a flat nosed projectile is a less efficient penetrator than a hemispherical nosed projectile of equal weight. A small increase in resistance to penetration is observed for an increased L/D ratio.

The Sandia equation (Young 1967, 1972) and the spherical cavity expansion technique (Ross and Hanagud 1969) were two penetration solutions considered for their applicability to frozen soil targets. Both methods produce good results at velocities below 600 m/s.

## TEST PROGRAM

The laboratory tests discussed here were conducted in the CRREL Terminal Ballistics Facility (Fig. 1) during July 1979. Testing consisted of firing small caliber (7.9-mm-diam) cylindrical projectiles into frozen Hanover silt targets, and measuring the impact velocities and projectile penetrations.

Four types of cylindrical steel projectiles were tested (Fig. 2), two with hemispherical noses, the other two flat-nosed. There was a long (L/D = 4) and a short (L/D = 2) version of each. Projectile data are summarized in Table 1.

Each projectile was inserted into a plastic sabot and then attached to a charged cartridge case (Fig. 3). A range of impact velocities were obtained by varying the propellant weight. Propellant data are shown in Figure 4.

The targets consisted of Hanover silt soil in 30.5-cm-square by 30.5-cm-deep boxes. Characteristics of the soil are shown in Figure 5. The soil was compacted in ten 2.5-cm-thick layers. Each layer was frozen at a temperature of  $-15^{\circ}\text{C}$  before the next layer was added to

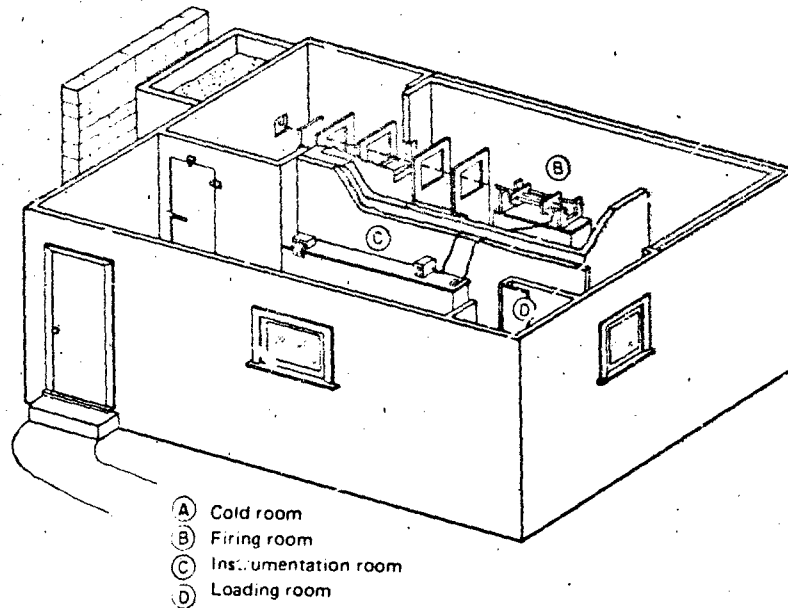


Figure 1. CRREL terminal ballistics facility.

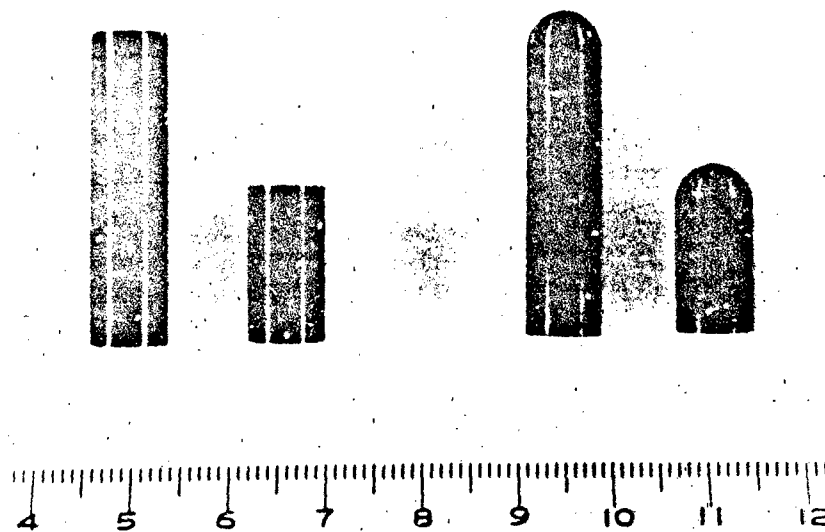


Figure 2. Projectiles tested (scale in cm).

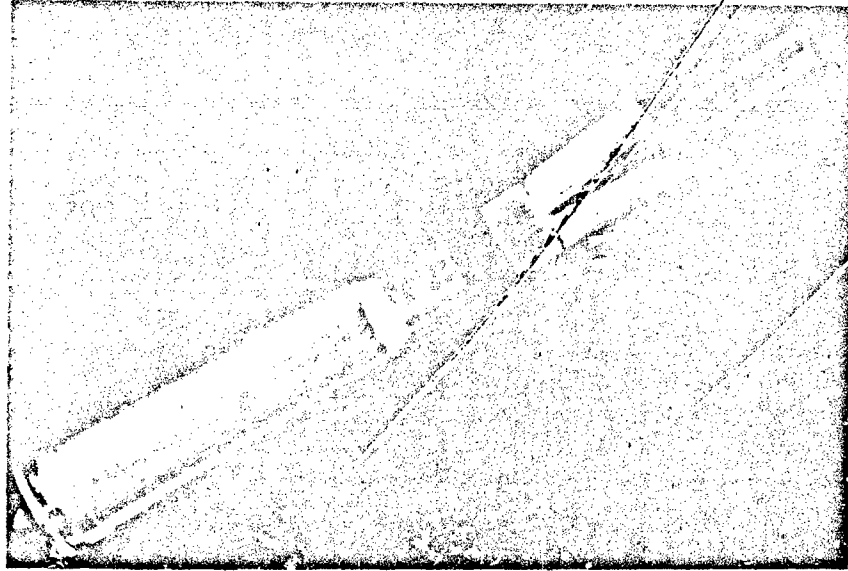


Figure 3. Test round components. L to R: cartridge, sabot, cylindrical projectile (flat nose) (scale in cm).

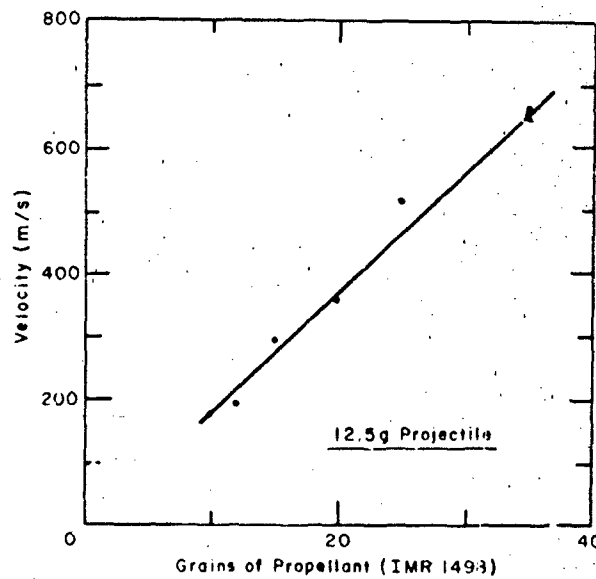


Figure 4. Propellant load versus velocity data.

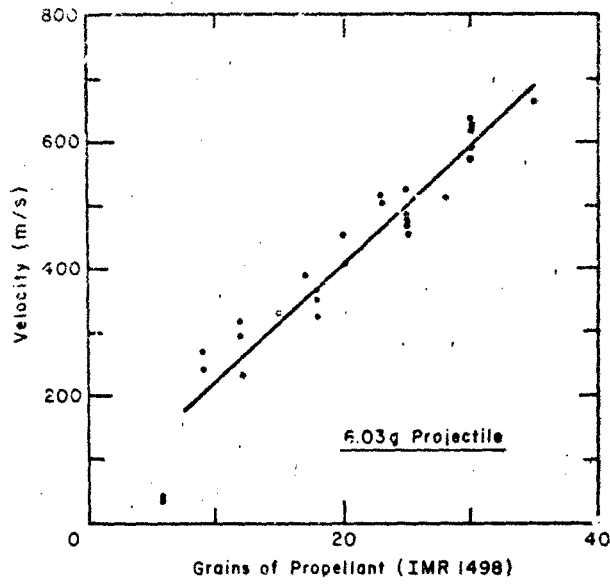


Figure 4. (cont'd.) Propellant load versus velocity data.

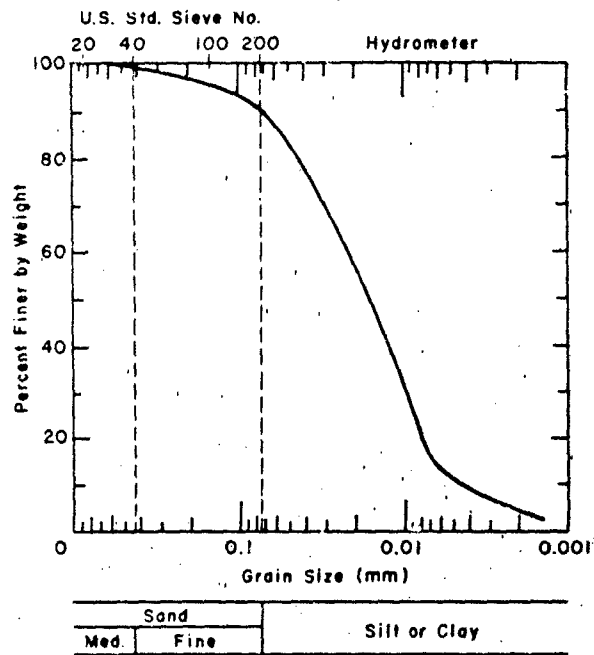


Figure 5. Characteristics of the Hanover silt used as a target material (LL=44.8, PL=non plastic, optimum water content=21.0%,  $G_s=2.69$ ).

Table 1. Description of projectiles.

<u>Nose shape</u>	<u>Length</u> (cm)	<u>Diam</u> (cm)	<u>L/D ratio</u>	<u>Mass</u> (g)
Hemisphere	1.7	0.7874	2.15	6.03
Hemisphere	3.3	0.7874	4.17	12.05
Flat	1.6	0.7874	2.02	6.03
Flat	3.2	0.7874	4.05	12.05

Material: Steel AISI C-1215

minimize moisture migration. Thermocouples were placed in the center and 2.5 cm from one side of the target during preparation.

The tests were conducted with the targets at temperatures of  $-10^{\circ}\text{C}$  and  $-25^{\circ}\text{C}$ . The targets were stabilized at the desired temperature for 24 hours before firing. Preparatory to firing, the target was turned on its side such that projectile penetration was perpendicular to the soil layers.

The projectiles were fired from a .350 Magnum Model 700 Remington bolt action rifle. They were fired through two pairs of chronograph screens, located such that projectile velocity was measured 1.5 m from the muzzle and 0.5 m in front of the target (3.5 m from the muzzle). The projectiles also passed through a paper witness screen, placed 20 cm in front of the target, which was used to determine projectile orientation.

After each shot, the target was moved so that approximately 5 to 8 cm of undisturbed soil was left around each impact area. To reduce any bias in the data from local target anomalies, different types of projectiles were selected randomly for firing into each target at the  $-10^{\circ}\text{C}$  test temperature. However, since only one target remained when the  $-25^{\circ}\text{C}$  testing began, only the short ( $L/D = 2$ ), flat-nosed projectiles were used so that as much data as possible could be obtained for one type projectile at this temperature.

After 11 to 12 projectiles were fired, the target box was disassembled by removing two of its sides. Each layer of soil was inspected and depth of penetration measurements were made normal to the target face. Soil samples were taken at representative locations for water content determination.

## DISCUSSION OF RESULTS

### General

A total of 57 projectiles were fired into five targets of frozen Hanover silt. Test results are summarized in Table 2.

Table 2. Penetration data.

Date 1979	Round	Projectile type <sup>a</sup>	Velocity (m/s)		Penetration depth (cm)	Remarks
			1.5 m <sup>b</sup>	0.5 m <sup>c</sup>		
Target 5: density 1.7 g/cm <sup>3</sup> , water content <sup>d</sup> 19.4% temperature -8.5°C at start, -9.1°C at finish						
10 July	1	LF	524	511	8.4	
	2	SF	420	410	6.4	
	3	LR	491	484	8.9	Yaw at impact
	4	SR	408	399	5.4	Yaw at impact
	5	LF	441	493	7.9	Tumbled in flight
	6	SF	472	464	-	Lost
	7	LR	468	548	7.9	Yaw at impact
	8	SR	464	456	12.4	e
11 July	9	SR	632	623	15.9	
	10	LF	668	661	22.4	
	11	SF	588	577	11.9	
	12	LR	655	640	-	Tumbled in flight
Target 4: density 1.7 g/cm <sup>3</sup> , water content <sup>d</sup> 18.4% temperature -11.2°C at start, -10.7°C at finish						
12 July	13	LF	346	282	4.4	Yaw at impact
	14	SF	346	277	4.9	
	15	LR	347	270	-	Tumbled in flight
	16	SR	347	318	5.4	
	17	LF	651	645	20.4	
	18	SF	651	638	9.4	
	19	LR	595	590	8.4	Yaw at impact
	20	SR	477	470	10.9	
	21	LR	347	234	-	Tumbled in flight
	22	LR	368	360	-	Tumbled in flight
	23	LR	347	246	-	Tumbled in flight
Target 3: density 1.7 g/cm <sup>3</sup> , water content <sup>d</sup> 19.0% temperature -11.7°C at start, -11.1°C at finish						
16 July	24	SF	-	268	2.4	
	25	LF	349	196	3.9	
	26	SR	-	241	2.4	
	27	LR	-	294	-	Tumbled in flight
	28	SF	497	484	6.9	
	29	LF	355	354	10.4	
	30	SR	348	326	5.6	
	31	LR	362	361	10.4	
	32	LR	503	498	14.4	Yaw at impact
	33	LF	349	292	7.4	
34	LR	349	319	6.4	Yaw at impact	

Table 2. (Continued)

Date 1979	Round	Projectile type <sup>a</sup>	Velocity (m/s)		Penetration depth (cm)	Remarks
			1.5 m <sup>b</sup>	0.5 m <sup>c</sup>		
Target 2: density 1.7 g/cm <sup>3</sup> , water content <sup>d</sup> 19.7% temperature -12.4°C at start, -11.9°C at finish						
17	35	LF	426	406	-	Tumbled in flight
July	36	SF	174	38	1.5	
	37	LF	555	547	16.4	Yaw at impact
	38	SR	187	38	1.0	
	39	LF	478	470	10.9	Yaw at impact
	40	SF	597	583	8.9	
	41	SR	542	-	9.9	Impact velocity lost
	42	SF	526	515	8.4	
	43	SR	487	480	9.4	
	44	SF	399	388	5.4	
	45	SR	466	459	10.4	

Target 6: density 1.7 g/cm<sup>3</sup>, water content<sup>d</sup> 19.1%  
temperature -24°C at start, -23.8°C at finish

19	46	SF	228	-	-	Yaw at impact
July	47	SF	105	-	-	Yaw at impact
	48	SF	347	296	3.4	
23	49	SF	349	325	4.4	
July	50	SF	361	354	5.4	
	51	SF	-	364	5.4	
	52	SF	531	519	6.9	
	53	SF	527	515	6.9	
	54	SF	651	635	8.9	
	55	SF	672	661	9.4	f
	56	SF	354	-	6.4	Impact velocity lost
	57	SF	540	527	8.4	

a. S(short), L/D = 2; L(long), L/D = 4; F = flat-nose, R = hemispherical nose.

b. Measured from muzzle.

c. Measured from target.

d. Average of water content at representative locations.

e. Round 8 traveled through same hole as round 7.

f. Slight deformation in nose area of projectile.



Figure 6. Dissected target.

Early in the test program it was found that some projectiles did not remain stable during penetration. As an example, Figure 6 shows a large ( $L/D = 4$ ) projectile with a hemispherical nose that followed a curved path through the target, coming to rest parallel to the target face. A straight trajectory (through the target) would have resulted in deeper penetration. Projectiles which did not travel straight through the target left a hole larger than 0.8 cm in the witness screen, indicating that some amount of yaw\* was occurring. It appeared that the yaw angle of the projectile at impact determined its penetration path through the target.

Projectile yaw can be induced by improper separation of the sabot from the projectile. In an attempt to obtain a higher percentage of stable projectile flights, thus increasing the number of near normal impacts, a series of modifications were made to improve sabot separation. Shown in Figure 7 is the sabot used for the large ( $L/D = 4$ ) projectiles and the sequence of changes made. The smaller sabot, used only with the short ( $L/D = 2$ ) projectiles, is shown in Figure 8. Only one modification was made to these. The first change was based on the assumption that a vacuum was occurring between the projectile base and sabot. To alleviate this, cuts were made parallel to the base, and almost through the side. The small projectiles attained stable flight characteristics with this modification. The larger ( $L/D = 4$ ) projectiles, however, still needed improvement. The possibility was considered that due to the greater length, friction force between the sabot and the projectile was too strong to be equalized by air resistance. Cuts made along the length of

\* Yaw is defined as the angle between the axis of the projectile at any moment and the trajectory (Dictionary of U.S. Army Terms, AR 310-25, 25 September 1975).

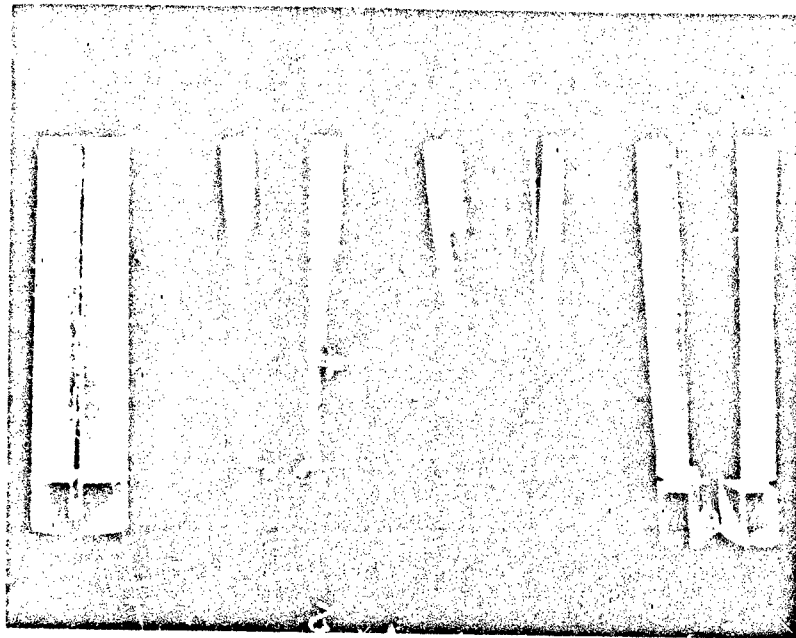
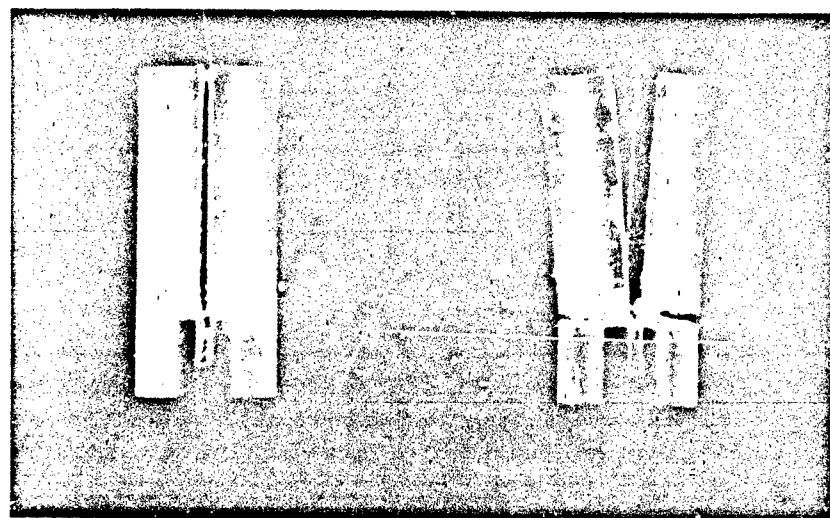


Figure 7. Large ( $L/D = 4$ ) projectile sabots and modifications.



5      6      7      8      9

Figure 8. Small ( $L/D = 2$ ) projectile sabots and modification (scale in cm).

the sabot, in addition to the first change, did not significantly improve the percentage of stable projectile flights. A final modification was to cut the sabot completely in half lengthwise. This modification, when combined with the earlier changes, increased the number of stable flights of the flat-nosed projectiles. The long, hemispherical-nose projectile flights were still mostly unstable, and after 14 of these projectiles were fired with only one normal impact their testing was discontinued. Even with the above modifications, a few projectiles of each type still did not impact normal to the target face.

Data from projectiles that showed signs of yaw or tumbling in flight were not included in the penetration versus impact velocity curves (Fig. 9-11).

#### Nose Shape Effect

Data from the short ( $L/D = 2$ ) projectiles are presented in Figure 9. These data indicate that the hemispherical-nosed projectiles were more efficient penetrators than the flat-nosed projectiles at impact velocities between 250 and 600 m/s. The relationship between depth of penetration of frozen soil and impact velocity is linear in this velocity region. It was found that within this velocity range cratering occurs during penetration. This cratering was independent of nose shape.

Two tests were conducted with impact velocities of 34 m/s, one for each of the two nose shapes. No cratering was observed in these tests, indicating that more efficient penetration was occurring at this velocity. Since the mechanics of penetration appear different in this velocity range the 34-m/s data were not included in the analysis.

These test results show that for impact velocities between 250 and 600 m/s, flat-nose projectiles are less efficient penetrators by about a factor of 1.4. The dashed curve in Figure 9 represents 1.4 times the penetration of the flat-nose projectiles. Based on least squares curve fits, the relation between the penetration of the hemispherical nose projectiles,  $P_H$ , and the flat-nose projectiles,  $P_F$ , is

$$P_H = 1.51 + 0.56 P_F$$

for impact velocities between 250 and 600 m/s.

A visual inspection of the frozen soil after projectile penetration did not reveal any differences in the penetration mechanics of the flat and hemispherical nose shapes. The soil had not closed in behind the projectile and the projectile path was polished as if some local melting and/or compaction had occurred during penetration. The soil in front of the projectiles did not appear disturbed or compacted.

#### L/D Influence

The effect of the  $L/D$  ratio is illustrated in Figure 10, where data for flat-nosed projectiles are presented. Comparison of these data

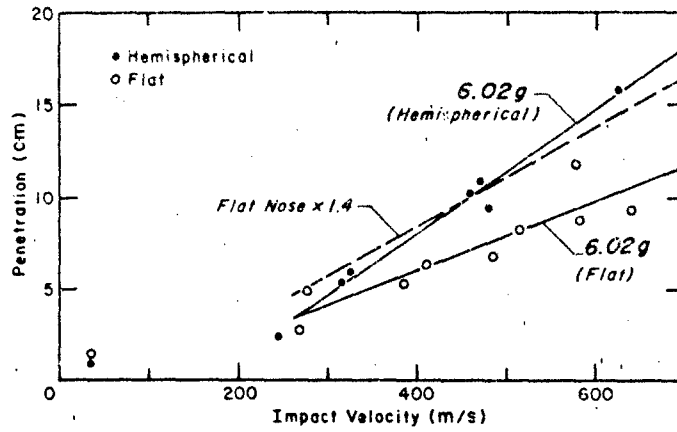


Figure 9. Nose shape influence on penetration of equal mass projectiles (the solid lines are least square curve fits to the data).

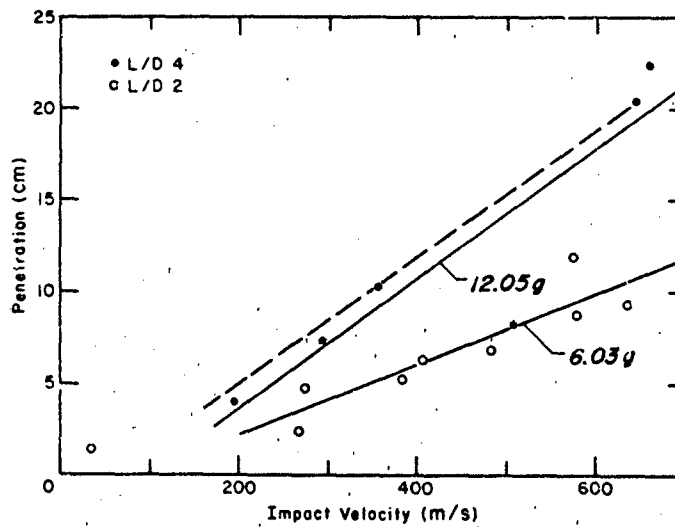


Figure 10. Effect of L/D ratio and mass on flat nose projectile penetration (the solid lines are least square curve fits to the data).

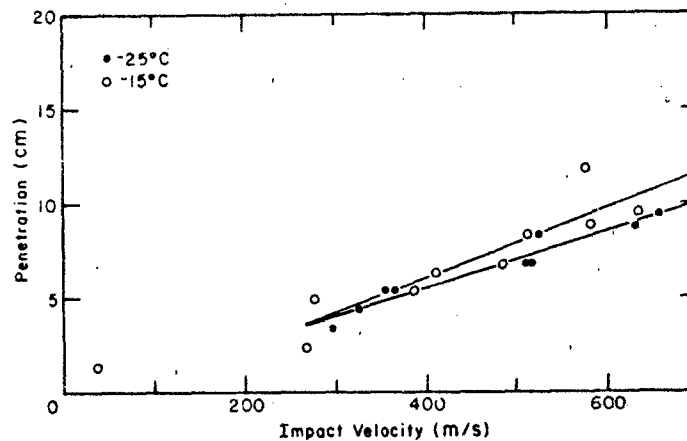


Figure 11. Effect of frozen soil temperature on projectile penetration (the solid lines are least square curves fits to the data).

reveals that the longer, heavier ( $L/D = 4$ ) projectiles penetrated deeper. These projectiles differ in both mass and  $L/D$  ratio, and since the mass of the larger (12.05-g) projectile is twice that of the smaller (6.03 g), it has twice the available energy for a given velocity. The dashed line in Figure 10 represents twice the penetration depth of the smaller projectile. The relative location of these curves suggests that the increase in  $L/D$  ratio causes a small increase in resistance between the projectile and the frozen soil. This appears to be second order when compared to the effect of doubling the mass.

#### Target Temperature Effects

One group of flat-nosed ( $L/D = 2$ ) projectiles was fired into a target at a temperature of  $-25^{\circ}\text{C}$  to evaluate the influence of target temperature on penetration. The resulting data are presented in Figure 11. Data from tests conducted at  $-10^{\circ}\text{C}$  with the same type projectile are also shown. Comparisons of the data reveal approximately an 8% difference in penetration. This difference may be somewhat questionable due to the scatter present in the data, but is not unexpected when soil properties are considered. Decreasing temperature below  $-10^{\circ}\text{C}$  by  $10^{\circ}$  or  $15^{\circ}$  has little effect on the constitutive properties of frozen soil as indicated by data presented by Tice (1976) and Stevens (1975). A more significant change in soil properties is seen by varying temperature between  $0^{\circ}$  and  $-10^{\circ}\text{C}$ . This suggests that greater penetration differences would be observed if higher temperatures were used.

#### PENETRATION ESTIMATES

##### General

Two methods of predicting projectile penetration into earth media are the Sandia equation (Young 1967, 1972) and the spherical cavity

expansion theory (Ross and Hanagud 1969). The Sandia equation was empirically derived from an extensive data base of large penetrator tests in unfrozen soil. Accurate predictions are dependent on the ability of the user to select appropriate coefficients for different impact conditions. By estimating these coefficients, upper and lower bounds of projectile penetration depth can be predicted.

The spherical cavity expansion solution was developed from equations based on the expansion of a cavity caused by penetration of a target by a sphere. This equation utilizes target parameters obtainable from standard laboratory strength tests.

Further discussions of the merits of the two approaches are presented by Aitken (1978) and Hadala (1975).

These two prediction methods were applied to frozen soil and snow targets by Aitken (1978). He found that the Sandia equation performed well in frozen soil but not snow, and that the reverse was true for the spherical cavity expansion solution.

#### Sandia Equation

The Sandia equation for impact velocities greater than 60 m/s is

$$D = 0.0117 KSN \sqrt{W/A} (V - 30.5) \quad (1)$$

where

- D = maximum penetration depth, m
- K = mass scaling coefficient, dimensionless
- S = soil constant, dimensionless
- N = nose shape coefficient, dimensionless
- W = projectile weight, kg
- A = projectile area, cm<sup>2</sup>
- V = impact velocity, m/s

The three coefficients K, S, and N are defined for various soils, nose shapes and projectile masses by Young (1972). The nose shape and soil coefficients are shown in Tables 3 and 4. Young does not present data on the mass scaling factor for projectiles smaller than 2 lb (0.91 kg). Aitken (1978), proposed an equation for a mass scaling factor applicable to projectiles weighing less than 0.9 kg:

$$K = .073 e^{.224 \ln W} \quad (2)$$

A preliminary estimate of total penetration for the (L/D = 2) projectiles with flat noses using eq 1 and 2 revealed that with a soil constant of 2, penetration into the -10°C target was underestimated, and conversely, penetration was overestimated for the -25°C target. As indicated in Table 4, S ranges between 1 and 3 for frozen soil, and stronger materials have lower soil constants. As previously discussed,

Table 3. Nose performance coefficient (after Young 1972).

<u>Nose shape</u>	<u>Nose caliber<sup>(a)</sup></u>	<u>N</u>
Flat	0	0.56
Hemisphere	0.5	0.65 <sup>(b)</sup>
Cone	1	0.82 <sup>(b)</sup>
Tangent ogive	1.4	0.82
Tangent ogive	2	0.92
Tangent ogive	2.4	1.0
Cone	2	1.08
Tangent ogive	3	1.11
Tangent ogive	3.5	1.19
Step cone	3	1.28
Biconic	3	1.31
Cone	3	1.33

(a) Nose caliber = nose length ÷ nose base diameter.

(b) Estimated by Young.

only a small temperature effect on depth of penetration was found, with less penetration occurring in the lower temperature soil. The soil constants were adjusted to reflect this fact. Shown in Figures 12 and 13 are solutions of eq 1 compared with the actual test results. These estimates were obtained using S values of 1.9 and 2.1 for -25°C and -10°C Hanover silt, respectively.

Two solutions of the Sandia equation using different nose shape coefficients are compared with actual test results in Figure 14. Young (Table 3) estimates that for a hemispherical nose shape the nose coefficient is 0.65; however, a somewhat closer agreement with test results (using the method of least squares) is obtained if a value of 0.77 is used for N. Thus a more appropriate value for the nose-shape coefficient, based on these test data, may be somewhat greater than 0.65.

The remaining test data to be compared with the Sandia equation are the flat nose, L/D = 4 data, which are shown in Figure 15; again two Sandia solutions are shown. Soil and nose shape factors of 2.1 and 0.56 are used. A mass scaling factor of 0.13 obtained from eq 2 was first used, but a more accurate prediction resulted from using a value of 0.14. This, along with refinements of the soil constant, led to a recalculation of Aitken's mass scaling equation. The revised equation (eq 3) is plotted in Figure 16, and is an excellent fit to the data:

$$K = .0772 e^{.215 \ln W} \quad (3)$$

This equation does not produce results significantly different than eq 2, but does reflect utilization of the additional data obtained from the above tests as well as refinements in the soil constant selections.

Spherical Cavity Expansion Technique

The spherical cavity expansion solution to projectile penetration utilizes target parameters determined by laboratory-tests to estimate penetration. Additionally, a major assumption of the solution is that the target material behaves as a locked-elastic, locked-plastic material as shown in Figure 17. The equation is:

Table 4. Typical soil constants for natural earth materials (after Young 1972)

<u>Soil constants</u>	<u>Materials</u>
0.2 - 1	Massive medium to high strength rock, with few fractures. Concrete, 2000 to 5000 psi, reinforced.
1 - 2	Frozen silt or clay, saturated, very hard. Rock, weathered, low strength, fractured. Sea or fresh-water ice more than 10 ft thick.
2 - 3	Massive gypsite deposits (WSMR). Well cemented coarse sand and gravel. Caliche, dry. Frozen moist silt or clay.
4 - 6	Sea or freshwater ice from 1 to 3 ft thick. Medium dense, medium to coarse sand, no cementation, wet or dry. Hard, dry dense silt or clay (TTR dry lake playas). Desert alluvium.
8 - 12	Very loose fine sand, excluding topsoil. Moist stiff clay or silt, medium dense, less than about 50% sand.
10 - 15	Moist topsoil, loose, with some clay or silt. Moist medium stiff clay, medium dense, with some sand.
20 - 30	Loose moist topsoil with humus material, mostly sand and silt. Moist to wet clay, soft, low shear strength.
40 - 50	Very loose dry sand topsoil (Eglin AFB). Saturated very soft clay and silts, with very low shear strengths and high plasticity (Great Salt Lake Desert and bay mud at Skaggs Island). Wet lateritic clays.

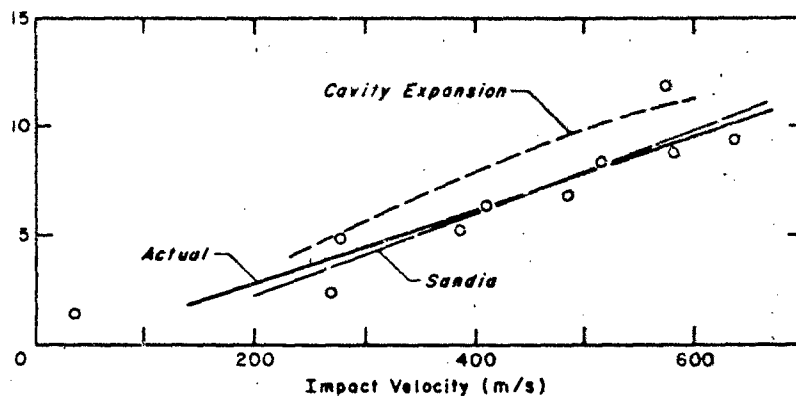


Figure 12. Comparison of test data with penetration solutions, for the flat-nose,  $L/D = 2$  projectile, target at  $-10^{\circ}\text{C}$ .

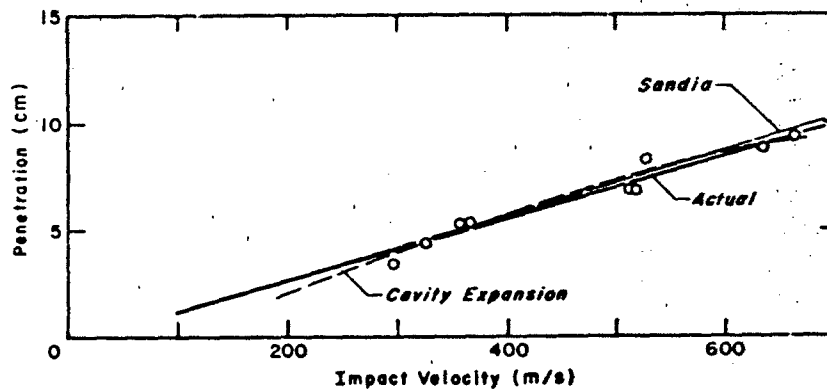


Figure 13. Comparison of test data with penetration solutions, for the flat-nose,  $L/D = 2$  projectile, target at  $-25^{\circ}\text{C}$ .

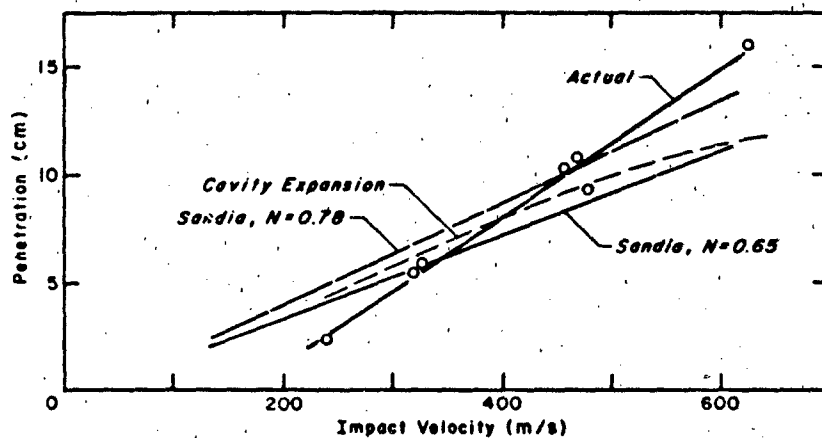


Figure 14. Comparison of test data with penetration solutions, for the hemispherical nose,  $L/D = 2$  projectile, target at  $-10^{\circ}\text{C}$ .

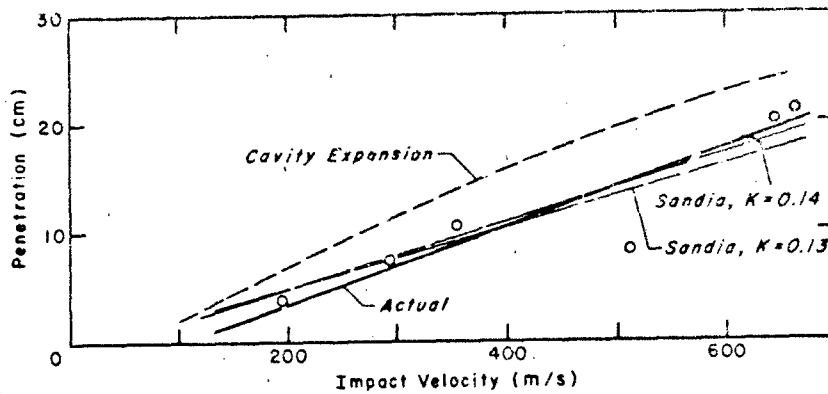


Figure 15. Comparison of test data with penetration solutions, for the flat-nose,  $L/D = 4$  projectile, target at  $-10^{\circ}\text{C}$ .

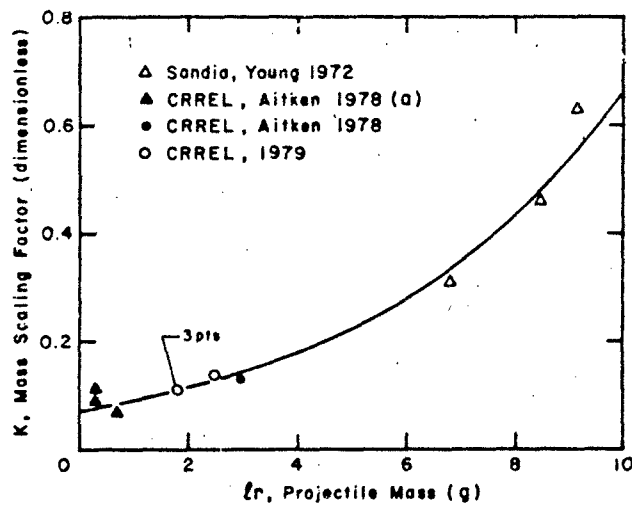


Figure 16. Relation between projectile mass and mass scaling factor  $K$ . a) Soil constant of 2.1 for Hanover silt at  $-10^{\circ}\text{C}$ .

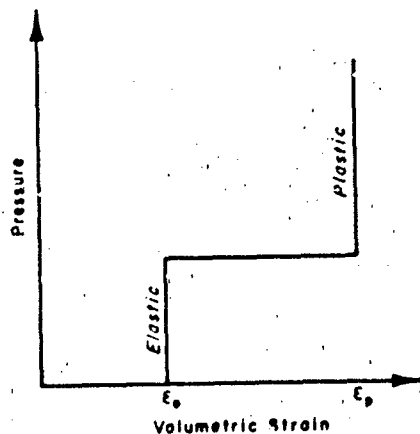


Figure 17. Idealized strain curve for spherical cavity expansion theory.

$$P = \frac{3W}{4Ag \rho_p B_2} + \frac{B_1 R}{2 B_2} \ln \left( 1 + \frac{2B_2 \rho_p V^2}{3B_3} \right) \quad (4)$$

where

V = velocity, ft/s  
P = penetration, ft  
W = projectile weight, lb  
A = projectile area, ft<sup>2</sup>  
g = acceleration of gravity, ft/s<sup>2</sup>  
R = projectile radius, ft  
ρ<sub>p</sub> = locked-plastic density of target material, slugs/ft<sup>3</sup>

and

$$\rho_p = \rho_o \exp(\Sigma_p) \quad (5)$$

where

ρ<sub>o</sub> = initial density of target material, slugs/ft<sup>3</sup>  
Σ<sub>p</sub> = plastic volumetric strain, %

and

$$B = \frac{y}{2E} - \frac{\Sigma_1}{3} \quad (6)$$

where

y = yield strength of target material, lb/ft<sup>2</sup>  
E = Young's modulus of target material, lb/ft<sup>2</sup>  
Σ<sub>1</sub> = elastic volumetric strain, %

$$\alpha_p = 1 - \frac{\rho_o}{\rho_p} \quad (7)$$

$$\delta = \alpha_p \exp(-3B) \quad (8)$$

$$B_1 = 1 - \delta^{1/3} \quad (9)$$

$$B_2 = 3/2 - (1 + \alpha_p) \delta^{1/3} + 1/2 \delta^{4/3} \quad (10)$$

$$B_3 = 4/9E [1 - \exp(-3B)] - 2/3 y \ln \delta + 2/27 \pi^2 E_c - 4/9 E_c \eta \quad (11)$$

where

$E_t$  = plastic modulus of deformation,  $\text{lb/ft}^2$

and

$$\eta = \sum_{n=1}^{\infty} \frac{\delta^n}{n^2} \quad (12)$$

$\Sigma_i$  and  $\Sigma_p$  describe the compressibility of the material idealized by the locked-elastic/locked-plastic behavior shown in Figure 17. In this application, it was assumed  $\Sigma_i = 0$  since, as pointed out by Rohani (1973), the elastic strains (i.e. the strains associated with the initiation of plastic deformation) for most soils are generally very small, indicating that  $\Sigma_i$  should also be small. Ross and Hanagud (1969) also state that  $\Sigma_i$  may be assumed zero without any loss in generality for most target materials. Rohani (1973) presents a parametric study which supports this assumption for materials with limited compressibility. The plastic volumetric strain  $\Sigma_p$  can be determined from an equation presented by Rohani (1973) which disregards any compressibility of the soil particles and water. Equating  $\Sigma_p$  to the specific volume of air, the equation is

$$\Sigma_p = V_{\text{air}} = \frac{e_o}{1+e_o} (1-S_o) \quad (13)$$

$$0 \leq S_o \leq 1$$

where

$e_o$  = void ratio

$S_o$  = degree of saturation

For the Hanover silt tested,  $e_o = 0.69$  and the saturation was 82%, yielding a value of 0.07 for  $\Sigma_p$ .

The following target strength and projectile parameters were used in the solution of eq 4:

$\rho_o = 106 \text{ lb/ft}^3$ , density of target (Table 2)

$V = 300$  to  $2000 \text{ ft/s}$

$Y = 3220$  ( $-10^\circ\text{C}$ ) and  $6,000 \text{ psi}$  ( $-25^\circ\text{C}$ ) (Aitken 1976)

$E = 215,000$  ( $-10^\circ\text{C}$ ) and  $400,000 \text{ psi}$  ( $-25^\circ\text{C}$ ) (Aitken 1976)

$E_t = 0$  (Aitken 1976)

$W = 1.33 \times 10^{-2}$  and  $2.66 \times 10^{-2} \text{ lb}$

$A = 5.2 \times 10^{-3} \text{ ft}^2$

$R = 1.29 \times 10^{-2} \text{ ft}$

The dashed lines in Figures 12-15 are the penetrations computed using the cavity expansion equation. It appears that these estimates agree with the test data except in Figure 15, where penetration for the flat-nosed  $L/D = 4$  projectile is overestimated. In Figure 14 the penetration estimate begins to diverge from the test data at an impact velocity of approximately 500 m/s. This can also be observed in data presented by Aitken (1978), for a spherical projectile with impact velocities up to 1000 m/s. His data show that at 1000 m/s the actual penetration is approximately twice the estimate. If the curves in Figure 14 were extended, similar results would be obtained, i.e. much higher penetrations than predicted at high impact velocities.

#### CONCLUSIONS

- 1) Using the test procedure described here, small sabotaged projectiles can be launched and can achieve stable flight. Near normal target impacts are then obtainable, and impact velocities are easily varied.
- 2) A projectile with a flat nose is a less efficient penetrator of frozen soil than one having a hemispherical nose.
- 3) Increasing the  $L/D$  ratio from 2 to 4, thus doubling the mass of a projectile, almost doubles the penetration. A small increase in resistance to penetration is also seen.
- 4) The Sandia equation, when used with the mass scaling equation recalculated here, accurately predicts small caliber projectile penetration into frozen soil at low velocities. Changes in nose shape and target strength can be accommodated by choosing the appropriate coefficients.
- 5) The hemispherical nose shape coefficient for the Sandia equation may be somewhat higher than the 0.65 estimated by Young (1972). Additionally, the soil constants for saturated frozen Hanover silt are 1.9 and 2.1 for soil temperatures of  $-25^{\circ}\text{C}$  and  $-10^{\circ}\text{C}$  respectively.
- 6) The spherical cavity expansion equation produces good results for impact velocities below 600 m/s, the limit of these tests.

LITERATURE CITED

- Aitken, G.W., G.K. Swinzow, and D.R. Farrell (1976) Projectile and fragment penetration in snow and frozen soil. Proceedings of the Army Science Conference.
- Aitken, G.W. (1978) Terminal ballistics in cold regions materials. Proceedings, Fourth International Symposium on Ballistics, October.
- Bernard, R.S. and S.V. Hangud (1975) Development of a projectile penetration theory, Report 1, Penetration theory for shallow to moderate depths. U.S. Army Engineers Waterways Experiment Station Technical Report 5-75-9.
- Hadala, P.F. (1975) Evaluation of empirical and analytical procedures used in predicting the rigid body motion of an earth penetrator. USAEWES MP 5-75-15.
- Rohani, B. (1973) Fragment and projectile penetration resistance of soils, Report 2, High velocity fragment penetration into laboratory-prepared soil targets. USAEWES MP 5-71-12.
- Ross, B. and S.V. Hanagud (1969). Penetration studies of ice with application to arctic and subarctic warfare. Prep. for Sub-Arctic Warfare and Science Program by Stanford Research Institute, Report 274-008.
- Stevens, H.W. (1975) The response of frozen soil to vibratory loads. CRREL Technical Report 265.
- Tice, A.R., D.M. Anderson, and A. Banin (1976) The prediction of unfrozen water contents in frozen soils from liquid limit determinations. CRREL Report 76-8.
- Young, C.W. (1967) The development of empirical equations for predicting depth of an earth penetrating projectile. Sandia Laboratories, SC-DR-67-60.
- Young, C.W. (1972) Empirical equations for predicting penetration performance in layered earth materials for complex penetrator configurations. Sandia Laboratories, SC-DR-72-0523.